



## Ce ions surface-modified TiO<sub>2</sub> aerogel powders: a comprehensive study of their excellent photocatalytic efficiency in organic pollutants removal

Guru Karthikeyan Thirunavukkarasu,<sup>a</sup> Olivier Monfort,<sup>a,\*</sup> Martin Motola,<sup>a</sup> Monika Motlochová,<sup>b</sup> Maroš Gregor,<sup>c</sup> Tomáš Roch,<sup>c</sup> Maria Čaplovicová,<sup>d</sup> Aleksandra Y. Lavrikova,<sup>e</sup> Karol Hensel,<sup>e</sup> Vlasta Brezová,<sup>f</sup> Monika Jerigová,<sup>g,h</sup> Ján Šubrt,<sup>b</sup> Gustáv Plesch<sup>a</sup>

## Electronic Supplementary Information

<sup>a</sup> Department of Inorganic Chemistry, Faculty of Natural Sciences, Comenius University in Bratislava, Ilkovicova 6, Mlynska Dolina, 842 15 Bratislava, Slovakia

<sup>b</sup> Institute of Inorganic Chemistry, Czech Academy of Sciences, Husinec-Rez c.p. 1001, 250 68 Rez, Czechia

<sup>c</sup> Department of Experiment Physics, Faculty of Mathematics, Physics and Informatics, Comenius University in Bratislava, Mlynska Dolina, 842 48 Bratislava, Slovakia

<sup>d</sup> STU Center for Nanodiagnostics, Slovak University of Technology in Bratislava, Vazovova 5, 812 43 Bratislava, Slovakia

<sup>e</sup> Division of Environmental Physics, Faculty of Mathematics, Physics and Informatics, Comenius University in Bratislava, Mlynska Dolina, 84248, Bratislava, Slovakia

<sup>f</sup> Institute of Physical Chemistry and Chemical Physics, Faculty of Chemistry and Food technology, Slovak University of Technology in Bratislava, Radlinskeho 9, 812 37 Bratislava, Slovakia

<sup>g</sup> International Laser Centre, Ilkovicova 3, 842 48 Bratislava, Slovakia

<sup>h</sup> Department of Physical and Theoretical Chemistry, Faculty of Natural Sciences, Comenius University in Bratislava, Ilkovicova 6, Mlynska dolina, 842 15 Bratislava, Slovakia

\* Corresponding author: monfort1@uniba.sk (email), +421(0)290142141 (phone)

**Calculation of percentage of anatase phase present in P25 sample:**

The P25 samples consist of ~82% of anatase phase, which is calculated using the formula <sup>1</sup>:

$$W_A = \frac{1}{1 + 1.26 \left(\frac{I_R}{I_A}\right)}$$

where,  $I_R$  and  $I_A$  is the strongest intensity of the rutile (110) and anatase (101) diffraction peak, respectively.

**Table S1:** Summary of Ce modified TiO<sub>2</sub> for photocatalytic application.

| Material   | Synthesis Technique         | Ce Dopant Concentration                                       | Bandgap (eV)  | Type of Pollutant  | Degradation % | Ref.          |
|--|-----------------------------|---|---|--|---------------|---------------|
| Ce <sup>3+</sup> -TiO <sub>2</sub> catalysts                                     | Sol-gel                     | 0.7% atomic ratio (Ce/Ti)                                     | Not calculated. But adsorption increased in the 400-500 nm region | <ul style="list-style-type: none"> <li>2-mercaptobenzothiazole</li> <li>Visible Light</li> <li>1.1 h</li> </ul>                  | 100           | <sup>2</sup>  |
| Ce-TiO <sub>2</sub>  | Sol-gel                     | 0.4wt% (Ce/TiO <sub>2</sub> )                                 | Not calculated. But adsorption increased in the 400-500 nm region | <ul style="list-style-type: none"> <li>Phenol</li> <li>UV light</li> <li>3 h</li> </ul>  | 100           | <sup>3</sup>  |
| Ce <sup>3+</sup> doped TiO <sub>2</sub>  | Precipitation               | 1.47wt% (EDX)   | 3.15  | <ul style="list-style-type: none"> <li>Orange II dye</li> <li>400 nm</li> <li>0.5 h</li> </ul>                                   | ~40           | <sup>4</sup>  |
| Mesoporous Ce/TiO <sub>2</sub>   | Sol-gel                     | 5 mol%  | Not calculated. But adsorption increased in the 400-500 nm region | <ul style="list-style-type: none"> <li>Methylene blue (MB)</li> <li>Visible light</li> <li>1 h</li> </ul>                        | 100           | <sup>5</sup>  |
| Cerium-doped SiO <sub>2</sub> /TiO <sub>2</sub> nanofibers                       | Sol-gel and electrospinning | 0.2% molar ratio (Ce/Ti)                                      | Not calculated. But adsorption increased in the 400-500 nm region | <ul style="list-style-type: none"> <li>Methylene blue (MB)</li> <li>Simulated sunlight</li> <li>2 h</li> </ul>                   | ~80           | <sup>6</sup>  |
| Ce doped TiO <sub>2</sub> nanosheets   | Hydrothermal                | 0.5% molar ratio  | ~3  | <ul style="list-style-type: none"> <li>Rhodamine B</li> <li>UV-Visible light</li> <li>1 h</li> </ul>                             | ~90           | <sup>7</sup>  |
| Ce- and S-co-doped TiO <sub>2</sub>  | Sol-gel                     | 0.04 g (Ce(NO <sub>3</sub> ) <sub>3</sub> ·6H <sub>2</sub> O) | 2.66  | <ul style="list-style-type: none"> <li>Acid Orange 7 (AO-7)</li> <li>Visible Light</li> <li>5 h</li> </ul>                       | 100           | <sup>8</sup>  |
| Ce/N co-doped TiO <sub>2</sub>   | Hydrothermal                | 0.05 g (Ce(NO <sub>3</sub> ) <sub>3</sub> ·6H <sub>2</sub> O) | 1.8   | <ul style="list-style-type: none"> <li>Acid Orange 7 (AO-7)</li> <li>Visible Light</li> <li>5 h</li> </ul>                       | 100           | <sup>9</sup>  |
| Sn/Ce co-doped TiO <sub>2</sub>  | Sol-gel                     | 2 mol%  | 3.02  | <ul style="list-style-type: none"> <li>Methylene blue (MB)</li> <li>Solar light</li> <li>2 h</li> </ul>                          | ~80           | <sup>10</sup> |
| Ce-TiO <sub>2</sub> P25  | Hydrothermal                | 0.29 mol% (Ce/TiO <sub>2</sub> )                              | 3.25  | <ul style="list-style-type: none"> <li>Methylene blue (MB)</li> <li>Visible light</li> <li>2.4 h</li> </ul>                      | ~96           | <sup>11</sup> |
| Ti <sup>3+</sup> -TiO <sub>2</sub> /Ce <sup>3+</sup> -CeO <sub>2</sub> nanosheet | Hydrothermal                | 1.56 at % (XPS)   | 2.7   | <ul style="list-style-type: none"> <li>Methyl orange (MO) and methylene blue (MB)</li> <li>Visible light</li> <li>3 h</li> </ul> | ~99           | <sup>12</sup> |
| In <sub>0.2</sub> -Ce <sub>0.2</sub> /TiO <sub>2</sub> aerogels                  | Sol-gel                     | 0.45 at%  | 2.84  | <ul style="list-style-type: none"> <li>Rhodamine B</li> <li>Visible</li> <li>1.5 h</li> </ul>                                    | ~96           | <sup>13</sup> |
| Ce doped TiO <sub>2</sub>  | Sol-gel                     | 0.5wt%  | 3.06  | <ul style="list-style-type: none"> <li>Caffeine</li> <li>Visible light</li> <li>2 h</li> </ul>                                   | ~30           | <sup>14</sup> |
| Ce-TiO <sub>2</sub> P25  | Hydrothermal                | 0.5wt% (Ce/Ti)  | 2.4   | <ul style="list-style-type: none"> <li>Methylene blue (MB)</li> <li>Visible light</li> <li>1.3 h</li> </ul>                      | ~90           | <sup>15</sup> |
| Ce-doped anatase TiO <sub>2</sub>  | Sol-gel                     | 0.1 mol%  | 3.31  | <ul style="list-style-type: none"> <li>Methylene blue (MB)</li> <li>UV light</li> <li>24 h min</li> </ul>                        | ~90           | <sup>16</sup> |

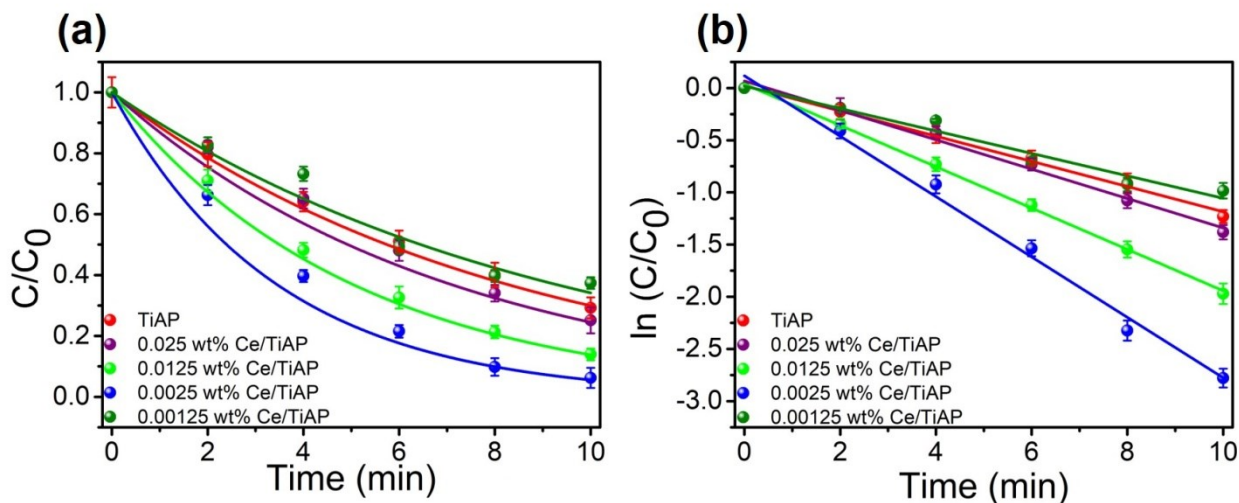


**Figure S1:** Influence of cerium ions surface-modification content on TiAP upon the photocatalytic efficiency in Rhodamine B decolorization under UVA light.

**Table S2:** The tabulation of photocatalytic activity rate ( $k$ ) and degradation % of Rhodamine B under UVA light with different concentration of cerium surface modification on TiAP.

| Sample              | Photocatalytic activity rate ( $k$ ) $\text{min}^{-1}$ | Degradation % |
|---------------------|--|---------------|
| TiAP                | 0.121  | ~71           |
| 0.025 wt% Ce/TiAP   | 0.141  | ~75           |
| 0.0125 wt% Ce/TiAP  | 0.198  | ~86           |
| 0.0025 wt% Ce/TiAP  | 0.289  | ~94           |
| 0.00125 wt% Ce/TiAP | 0.107  | ~63           |

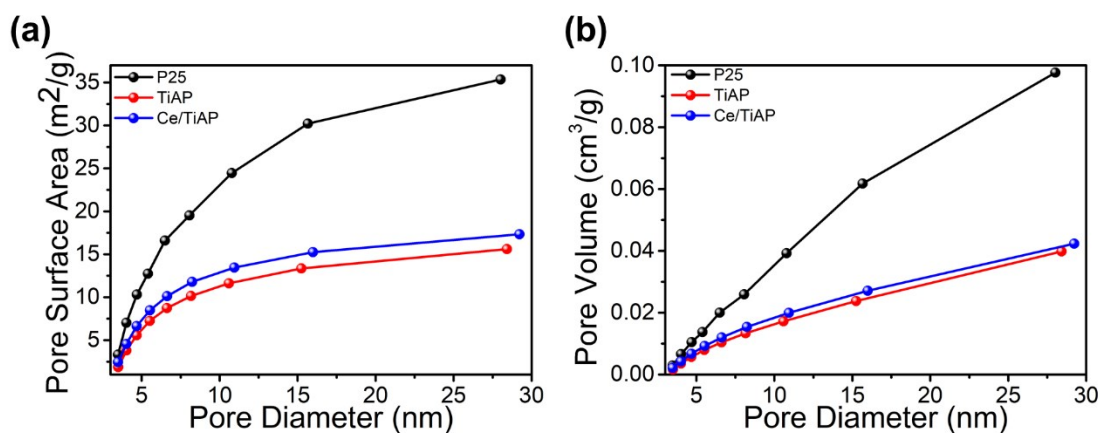


**Figure S2:** BET measurements of (a) Pore surface area and (b) pore volume respectively.

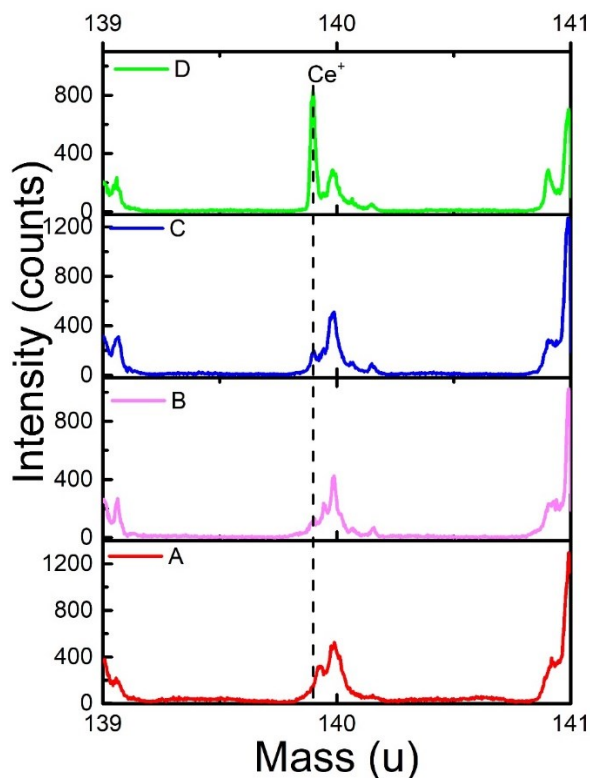


**Figure S3:** SIMS based detection of Ce in Ce/TiAP (A: Pristine TiAP, B: 0.00125 wt% Ce/TiAP, C: 0.0025 wt% Ce/TiAP and D: 0.0125 wt% Ce/TiAP).  $\text{Ce}^+$  ion peak was identified at 139.9 mu (dash line).

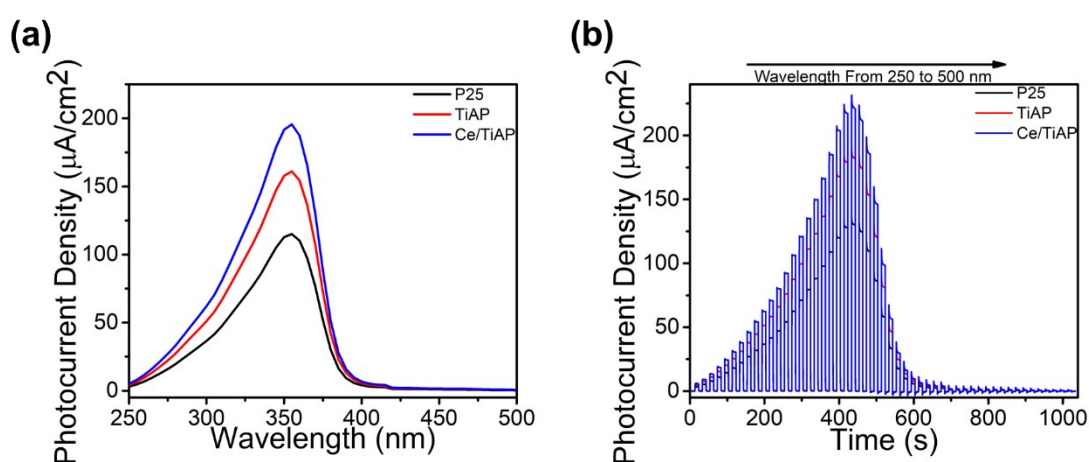


**Figure S4:** (a) Photocurrent densities of P25, TiAP and Ce/TiAP with (b) the corresponding transient current measured at 0.4  $V_{\text{Ag/AgCl}}$  in an aqueous 0.1 M  $\text{Na}_2\text{SO}_4$  solution in the spectral range from 300 nm to 500 nm.

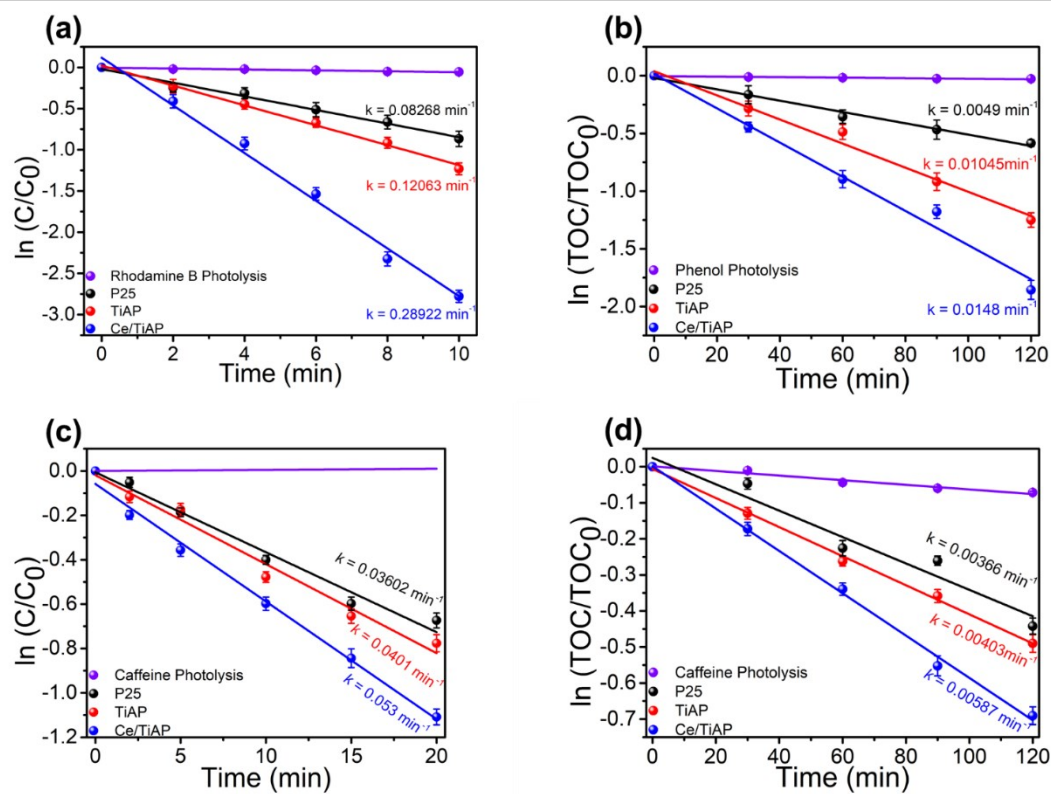


**Figure S5:** The linearized pseudo-first-order plots of  $\ln(C/C_0)$  versus time (a) Rhodamine B, (b) Phenol mineralization measured by total organic carbon content analyzer, (c) & (d) Caffeine degradation by HPLC and mineralization measured by total organic carbon content analyzer.

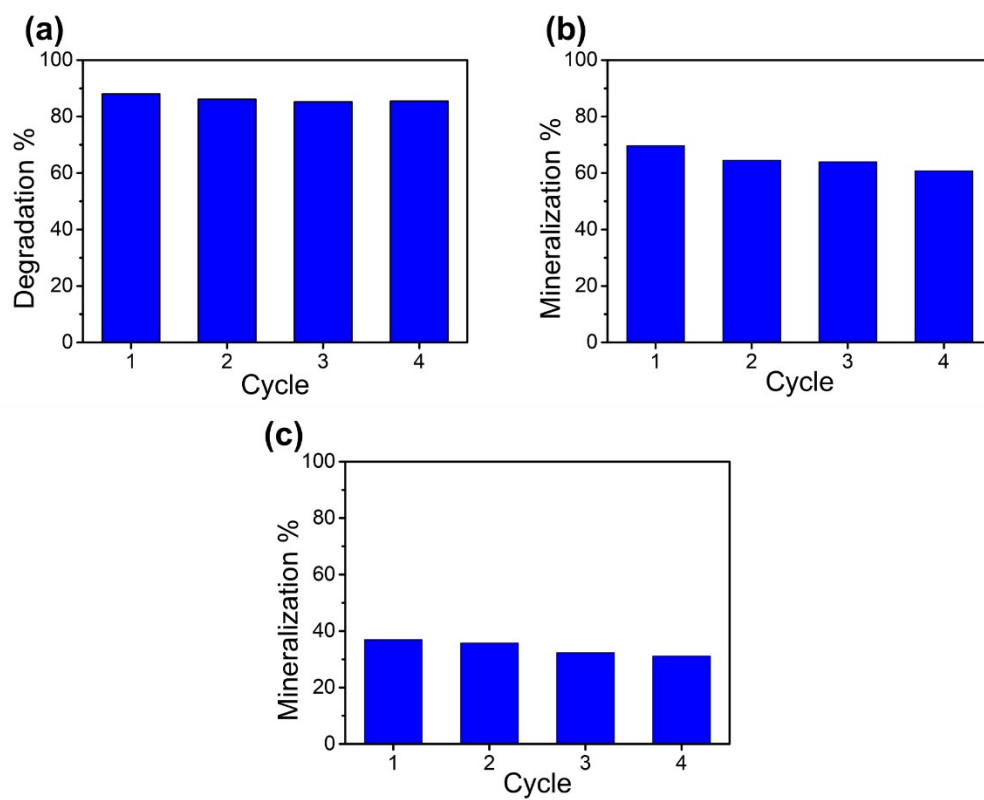


**Figure S6:** Repeated runs (4 cycles) using Ce/TiAP under UVA irradiation for the photocatalytic degradation of (a) Rhodamine B ( $C/C_0$ ), (b) Phenol (TOC), (c) Caffeine (TOC).

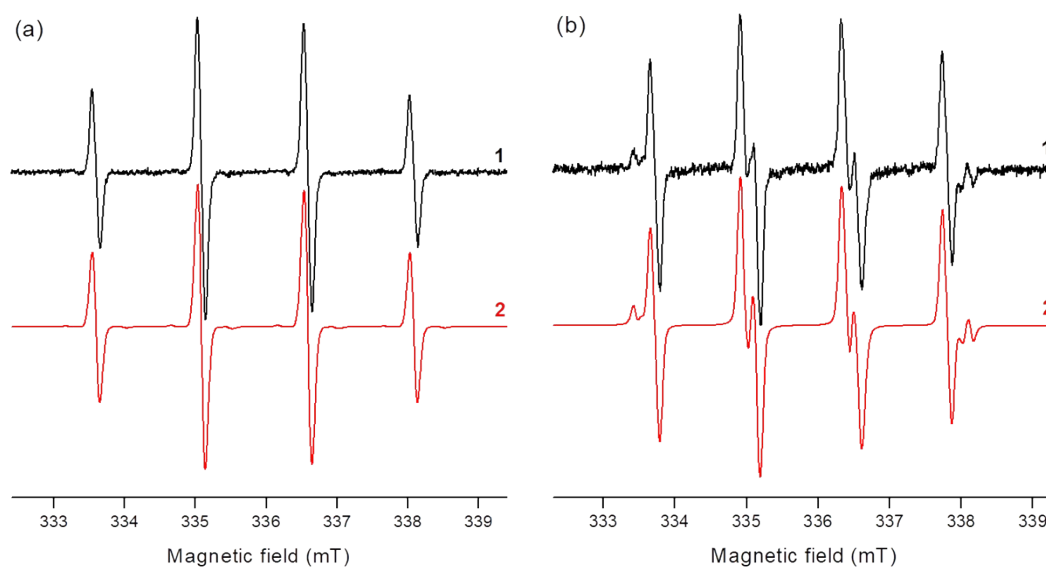


**Figure S7:** The normalized experimental (1) and simulated (2) EPR spectra obtained after 180 s exposure of aerated aqueous suspensions of TiAP in the presence of spin trapping agent: (a) DMPO; (b) BMPO. (LED@365 nm, irradiance 10 mW cm<sup>-2</sup>; TiO<sub>2</sub> loading 0.2 mg mL<sup>-1</sup>; c<sub>0</sub>(DMPO) = 0.04 M; c<sub>0</sub>(BMPO) = 0.02 M).

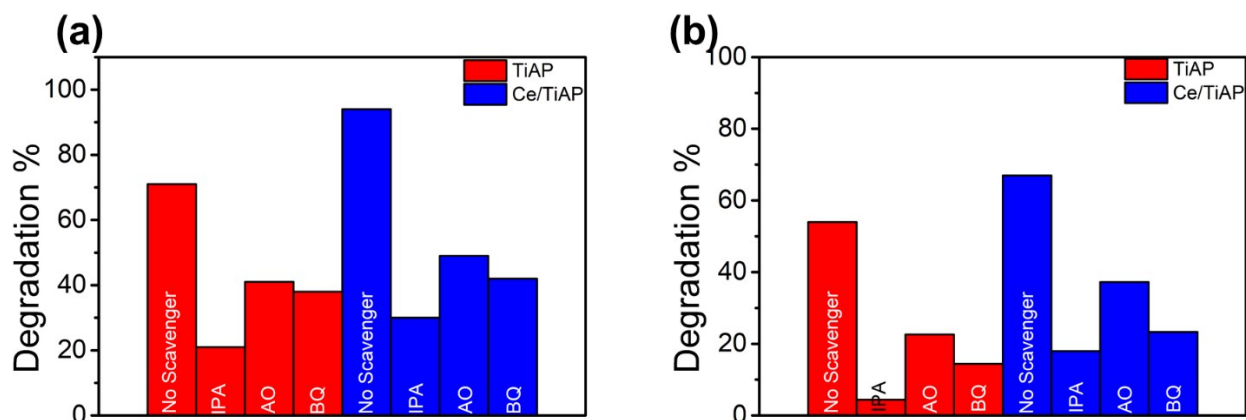


**Figure S8:** Free radical quenching of TiAP and Ce/TiAP using the isopropyl alcohol (IPA), ammonium oxalate (AO), benzoquinone (BQ) as scavengers (a) Rhodamine B and (b) caffeine.



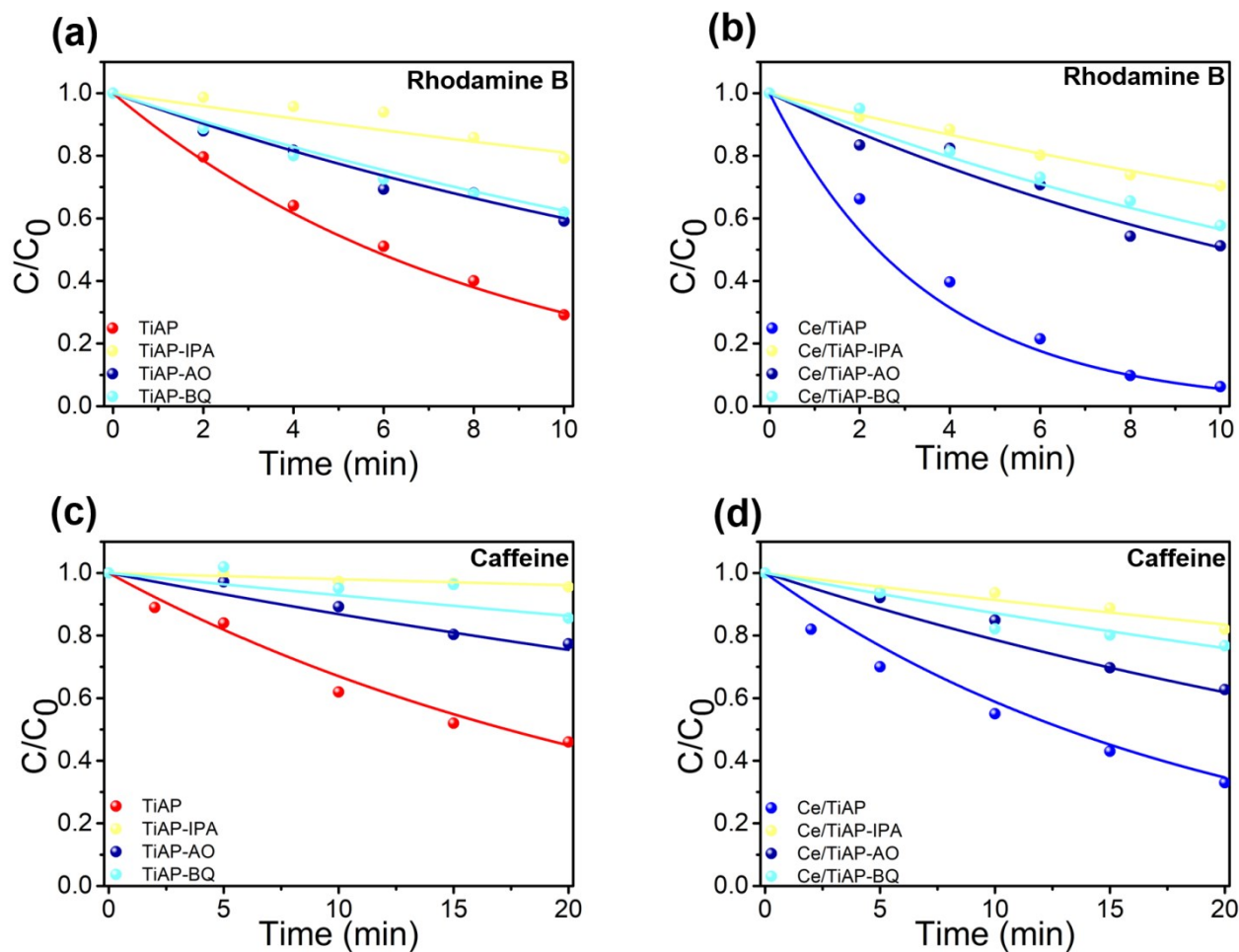


**Figure S9:** Degradation curves of (a) and (b) Rhodamine B and (c) and (d) Caffeine using TiAP and Ce/TiAP, respectively, under UVA irradiation.

## References

- 1 R. A. Spurr and Howard. Myers, *Anal. Chem.*, 1957, **29**, 760–762.
- 2 F. B. Li, X. Z. Li, M. F. Hou, K. W. Cheah and W. C. H. Choy, *Applied Catalysis A: General*, 2005, **285**, 181–189.
- 3 C. Fan, P. Xue and Y. Sun, *Journal of Rare Earths*, 2006, **24**, 309–313.
- 4 V. Štengl, S. Bakardjieva and N. Murafa, *Materials Chemistry and Physics*, 2009, **114**, 217–226.
- 5 N. Aman, P. K. Satapathy, T. Mishra, M. Mahato and N. N. Das, *Materials Research Bulletin*, 2012, **47**, 179–183.
- 6 Y. Liu, H. Yu, Z. Lv, S. Zhan, J. Yang, X. Peng, Y. Ren and X. Wu, *Journal of Environmental Sciences*, 2012, **24**, 1867–1875.
- 7 Y. Liu, P. Fang, Y. Cheng, Y. Gao, F. Chen, Z. Liu and Y. Dai, *Chemical Engineering Journal*, 2013, **219**, 478–485.
- 8 M. Nasir, Z. Xi, M. Xing, J. Zhang, F. Chen, B. Tian and S. Bagwasi, *J. Phys. Chem. C*, 2013, **117**, 9520–9528.
- 9 M. Nasir, S. Bagwasi, Y. Jiao, F. Chen, B. Tian and J. Zhang, *Chemical Engineering Journal*, 2014, **236**, 388–397.
- 10 M. Alijani and B. K. Kaleji, *Opt Quant Electron*, 2017, **49**, 34.
- 11 G. B. Vieira, H. J. José, M. Peterson, V. Z. Baldissarelli, P. Alvarez and R. de Fátima Peralta Muniz Moreira, *Journal of Photochemistry and Photobiology A: Chemistry*, 2018, **353**, 325–336.
- 12 Z. Xiu, Z. Xing, Z. Li, X. Wu, X. Yan, M. Hu, Y. Cao, S. Yang and W. Zhou, *Materials Research Bulletin*, 2018, **100**, 191–197.
- 13 R.-R. Zheng, T.-T. Li and H. Yu, *Global Challenges*, 2018, **2**, 1700118.
- 14 V. O. Ndabankulu, S. Maddila and S. B. Jonnalagadda, *Can. J. Chem.*, 2019, **97**, 672–681.
- 15 G. B. Vieira, G. Scaratti, F. S. Rodembusch, S. M. De Amorim, M. Peterson, G. L. Puma and R. D. F. P. M. Moreira, *Environmental Technology*, 2019, 1–15.
- 16 G. Bahmanrokh, C. Cazorla, S. S. Mofarah, R. Shahmiri, Y. Yao, I. Ismail, W.-F. Chen, P. Koshy and C. C. Sorrell, *Nanoscale*, 2020, **12**, 4916–4934.